

Effect of T6-like and T5-like Heat Treatment on the Microstructure and Hardness of Cast and 3D-Printed Al-Si-Mg Alloy Systems

Ayrah Andrea M. Marterior¹, Carla Joyce C. Nocheseda²,
and Mary Donnabelle L. Balela^{1*}

¹Sustainable Electronic Materials Group, Department of Mining, Metallurgical, and Materials Engineering, College of Engineering, University of the Philippines Diliman, Quezon City 1101 the Philippines
²Metals Industry Research and Development Center (MIRDC), Department of Science and Technology, Taguig City 1631 the Philippines

Aluminum (Al) alloys A356 and AlSi10Mg of the Al-Si-Mg system, considered counterparts, possess high industrial value due to their high strength-to-weight ratio and excellent mechanical properties. A356 is manufactured by conventional processes like casting, whereas AlSi10Mg is used to additively manufacture A356 by direct metal laser sintering. T5 and T6 heat treatment are widely employed on cast and wrought Al alloys to increase their strength, hardness, and other mechanical properties. Since AlSi10Mg is a relatively novel material and 3D printing is a new manufacturing technique, the standard T5 and T6 heat treatment conditions cannot be directly used. As such, this work studied the effects of T6-like (solutionizing, quenching, aging) and T5-like (direct aging) heat treatment on the cast and 3D-printed Al-Si-Mg alloys. The hardness of cast A356 increased from 58.6 to 85.6 HV while retaining its dendritic microstructure under T6. Then again, the hardness decreased after T5-like heat treatment at 100–400 °C. 3D-printed AlSi10Mg under T6 showed visible microstructure coarsening with decreasing hardness from 115 to 96 HV (along the z-direction). Under T5, the hardness significantly reduced at 300–400 °C. Results show that even slight temperature or time changes during heat treatment produce varying results. Ultimately, this work contributes to developing more accurate heat treatment procedures for 3D-printed Al-Si-Mg systems.

Keywords: 3D printing, Al-Si-Mg, heat treatment, microstructure

INTRODUCTION

Additive manufacturing (AM) is a layer-by-layer process that produces complex components for aerospace, automotive, and medical industries. The parts are created through three-dimensional (3D) computer-aided design models, and data is then transferred to the AM software. This process allows complex parts to be 3D-printed

directly, quickly, cost-effectively, and efficiently. Accuracy is high, and production time is short compared to traditional manufacturing techniques (Dev Singh *et al.* 2021).

The American Society for Testing and Materials (ASTM) established seven AM processes, with powder bed fusion (PBF) being the most common metal powder-based technique (Cherdo 2019). In PBF, metal particles are fused using a laser or electron beam to form the component.

*Corresponding author: mlbalela1@up.edu.ph

Direct metal laser sintering (DMLS) is a laser-PBF process widely adopted for its high efficiency and precision. The powder particles are heated just below the melting temperature (*i.e.* sintered) until the two surfaces are fused. Due to the layer-by-layer nature of DMLS, each layer is considered a small cast stacked upon the previous one (Tamez and Taha 2021). Typical engineering alloys used in DMLS include titanium, nickel, steel, and aluminum (Al) (Piller *et al.* 2018).

Al alloys A356 (AlSi7Mg0.3) and AlSi10Mg are part of the Al-Si-Mg system known for their high strength-to-weight ratio, good ductility, and corrosion resistance. However, it is essential to note that their primary production routes differ – A356 is commonly produced by casting, whereas AlSi10Mg is 3D-printed through DMLS (Fiocchi *et al.* 2021; Lee 2013). Hence, they are considered counterparts of each other.

Heat treatments are usually performed on cast A356 to improve its mechanical properties. It involves heating and cooling to obtain recrystallization and microstructural changes, as well as remove impurities and defects during manufacturing. The T6 method is a well-established heat treatment method for Al alloys and involves [1] solutionizing, [2] quenching, and [3] artificial aging (Lee 2013; Chaudhury *et al.* 2011). It is typically employed on wrought alloys such as Al alloy 6061, but T6-like heat treatments are also explored on cast Al alloys such as A356 and F357 (Fiocchi *et al.* 2021; Chauhan 2017). It is named T6-like to distinguish it from conventional T6 heat treatment. Previous studies have shown that T6-like heat treatment improves the mechanical properties of cast A356 such as its ultimate tensile strength, yield strength, and hardness (Kim *et al.* 2021; Liu *et al.* 2017; Zhu *et al.* 2012).

On the other hand, a T6-like heat treatment was performed on 3D-printed AlSi10Mg to eliminate the anisotropic microstructure due to the layer-by-layer nature of the DMLS process (Girelli *et al.* 2019). However, Aboulkhair *et al.* (2015) observed that the T6-like heat treatment led to material softening and decreased hardness values of the 3D-printed AlSi10Mg alloy. This is also consistent with findings in the literature (Girelli *et al.* 2019; Yu and Wang 2018; Aboulkhair *et al.* 2015). With this, Fiocchi *et al.* (2021) suggested that T6 parameters, *i.e.* time and temperature, must be optimized if applied to 3D-printed Al-Si-Mg alloys. Moreover, other heat treatment routes for 3D-printed parts could be explored to achieve the desired mechanical performance.

The conventional T5 heat treatment involves direct annealing of Al alloy at relatively low temperatures (around 120–300 °C) to strengthen by precipitation hardening. This single-step method does not require prior

solutionizing (Fiocchi *et al.* 2020, 2021; Rosenthal and Stern 2016). Rosenthal and Stern (2016) found that T5 heat treatment of 3D-printed AlSi10Mg alloys at 200 °C increases its hardness while lower hardness was observed at 220–250 °C. While the treatment was still called T5, for clarity, any heat treatment applied to non-conventional Al alloys would be referred to as T5-like. T5-like heat treatment is relatively underreported in literature, though there is a growing interest in exploring its potential as a post-processing method for 3D-printed AlSi10Mg alloys (Fiocchi *et al.* 2021).

This study investigates the effect of two heat treatment routes on the microstructure and hardness of cast A356 and 3D-printed AlSi10Mg. The first route employs a T6-like heat treatment following the solutionizing, quenching, and artificial aging method. In the second route, a T5-like heat treatment is used, which involves directly aging the samples at elevated temperatures below the solutionizing temperature. This work explores the interactions between the types of heat treatment and manufacturing processes for Al alloys and how they influence the resulting microstructure and hardness.

MATERIALS AND METHODS

Sample Preparation

The 3D-printed and cast Al-Si-Mg samples were produced by DMLS and traditional casting methods, respectively. For the 3D-printed sample, pristine EOS AlSi10Mg powder with a 25–70- μm particle size distribution was used as raw material. It was then produced using the EOS DMLS M290 machine with a 250 mm x 250 mm x 300mm building platform and a 400W continuous Yb:YAG fiber. Standard process parameters specified by the manufacturer were employed (laser power: 305 W; scanning speed: 1010 mm/s; layer thickness: 0.05 mm; hatch distance: 1.1mm) (EOS 2021). The bulk sample was built in the z-direction (build direction), and the scanning direction (xy-direction) was rotated between consecutive layers. It was then cut into smaller sections with 5 mm x 5 mm x 1.5 mm dimensions. On the other hand, a commercially available cast A356 sample was then cut into smaller circular sections. Table 1 shows the chemical composition of the Al-Si-Mg samples.

Heat Treatment

T6-like heat treatment was employed on both cast and 3D-printed Al-Si-Mg samples with the following conditions: [1] solution heat treatment at 540 °C for 8 h, [2] water quenching to room temperature, and [3] subsequent artificial aging at 155 °C for 5 h. On the other

Table 1. Chemical composition of the Al-Si-Mg samples.

Element	Al	Si	Fe	Cu	Mn	Mg	Ni	Zn	Pb	Sn	Ti	Sr
AlSi10Mg ^a	Bal.	9–11	≤ 0.55	≤ 0.05	≤ 0.45	0.25–0.45	≤ 0.05	≤ 0.10	≤ 0.05	≤ 0.05	≤ 0.15	–
AlSi7Mg0.3	Bal.	6.95	0.15	≤ 0.01	≤ 0.02	0.34	–	≤ 0.01	–	–	≤ 0.07	≤ 0.001

^aAs indicated in EOS AlSi10Mg Material Data Sheet; corresponds to ASTM F3318

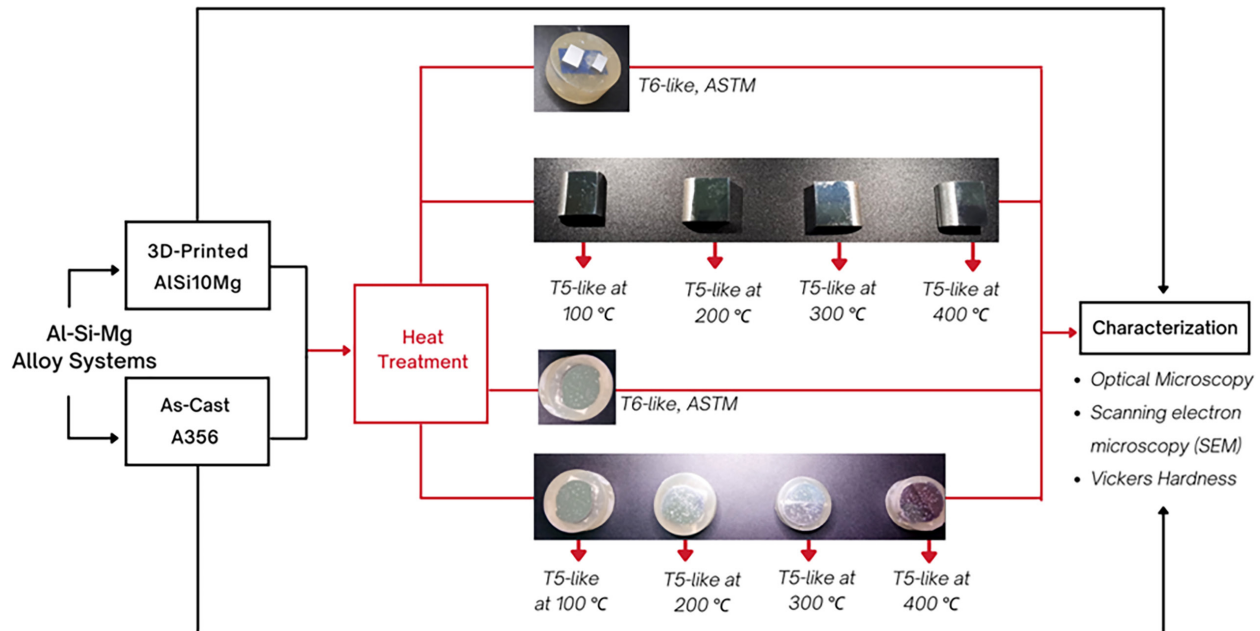


Figure 1. Experimental procedure for the heat treatment and characterization of the Al-Si-Mg samples.

hand, a T5-like heat treatment was performed for 2 h at 100, 200, 300, and 400 °C in a muffle furnace. Figure 1 illustrates the procedure for investigating the effects of heat treatment on the microstructure and mechanical properties of the Al-Si-Mg samples.

Characterization

Metallographic preparation was done on the smaller sections of the 3D-printed AlSi10Mg samples following ASTM E3-11. Surface grinding using SiC paper was employed, starting from a 120 grit size followed by 180, 240, 320, 400, until 600. These were then polished to a surface finish of 3 μm. Afterward, the polished samples were etched using 1% HF, and etching methods were performed according to ASTM E407-07. Microstructural analysis was done using a GX53 Olympus optical microscope at 100, 500, and 1000x magnifications. The microstructure of 3D-printed samples after T5-like heat treatment was analyzed using a Hitachi 3500 scanning electron microscope (SEM). For the cast samples, the microstructure was investigated using an optical microscope since the microstructure was large enough to be viewed under this microscope. The hardness values

were determined using a Vickers hardness tester at a load of 0.2gf. Five indentations were conducted, and the average hardness was obtained.

RESULTS AND DISCUSSION

Cast A356 Sample

Figure 2a shows the microstructure of the cast A356 alloy, consisting of α-Al dendrites with an interdendritic Al-Si eutectic. This follows the predicted microstructure below the eutectic temperature based on the equilibrium Al-Si phase diagram (Alkathafi *et al.* 2020; Birol 2009). After T6-like heat treatment, the alloy retained its dendritic morphology, as in Figure 2b. Interestingly, even with the same microstructure, the hardness increased from 58.6 (± 1.14) to 85.6 (± 13.63) HV after T6-like heat treatment. The exposure of cast A356 to elevated temperatures (540 °C) during the solutionizing step dissolved the soluble Si eutectic, leading to a more homogeneous distribution of Si in the α-Al matrix. The rapid quenching then resulted in a supersaturated solution that would trap defects, such

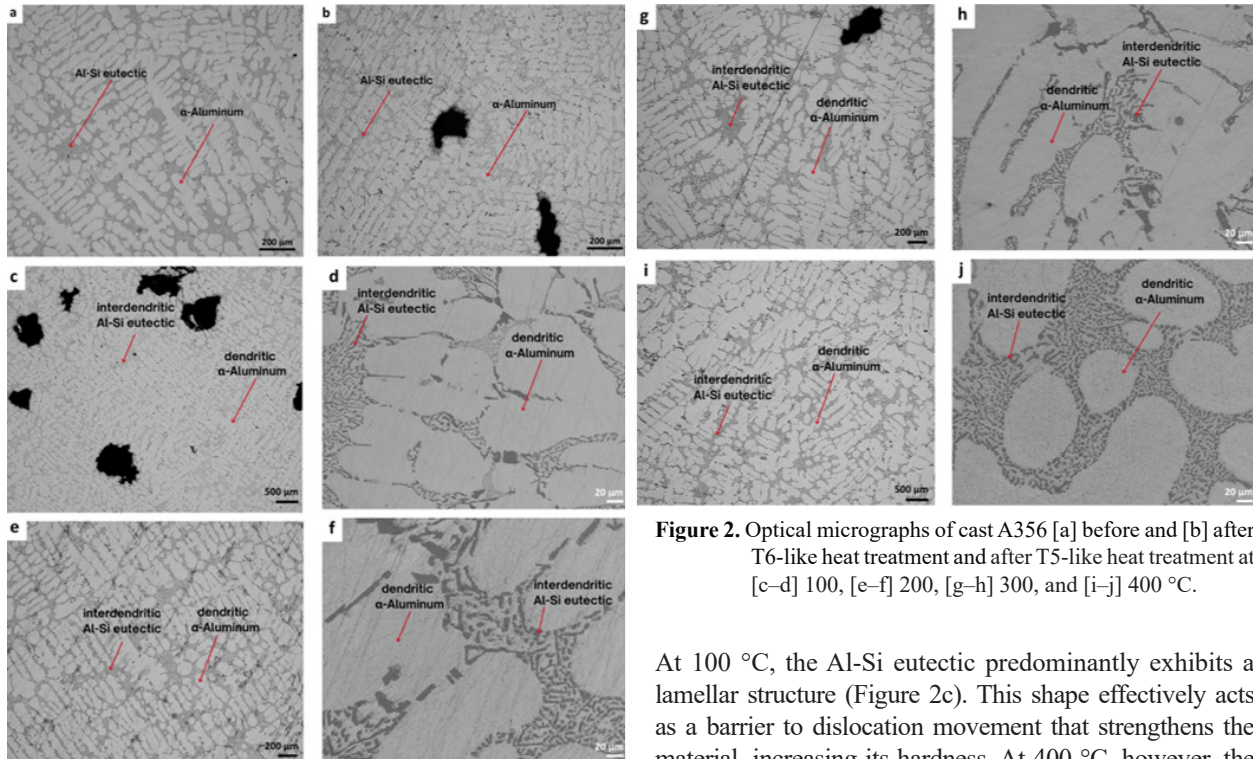


Figure 2. Optical micrographs of cast A356 [a] before and [b] after T6-like heat treatment and after T5-like heat treatment at [c–d] 100, [e–f] 200, [g–h] 300, and [i–j] 400 °C.

At 100 °C, the Al-Si eutectic predominantly exhibits a lamellar structure (Figure 2c). This shape effectively acts as a barrier to dislocation movement that strengthens the material, increasing its hardness. At 400 °C, however, the Al-Si eutectic showed more globular grains that reduced the density of interfaces. As a result, the hardness was lowered (Birol 2009). Figure 4a summarizes the effect of T5-like heat treatment on the microstructure and hardness of cast A356.

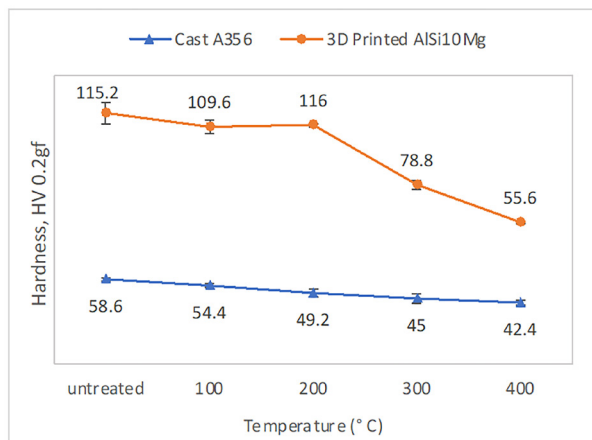


Figure 3. Effect of heat treatment on the hardness of cast and 3D-printed Al-Si-Mg samples after T5 heat treatments.

as vacancies and dislocations. These defects acted as nucleation sites for the growth of the α -Al dendrites during aging (Kim *et al.* 2021; Zhu *et al.* 2012).

The optical micrographs of the cast A356 after a T5-like heat treatment at 100–400 °C are shown in Figure 2c–j. All samples retained the dendritic α -Al and the Al-Si interdendritic eutectic. The dendrite size, estimated using ImageJ from the micrographs, increased from 241.22 to 262.87 μm as the temperature was raised from 100 to 400 °C. Then again, a corresponding reduction in the hardness with increasing temperatures was observed (Figure 3).

3D-Printed AlSi10Mg Sample

During the DMLS process, the laser scans a specific area to form each layer and leaves a mark called the scan track. Partial melting of the metal powder inside the scan track creates the melt pool. This scanned area is then subjected to fast cooling rates to ensure it adheres to the previous layer. It rapidly solidifies, and the high thermal gradient induces internal stresses in the built part (Aboulkhair *et al.* 2016).

Figure 5 shows the optical micrographs of the 3D-printed AlSi10Mg sample before and after T6-like heat treatment. Wave-like patterns formed along the build direction (z-direction) of the untreated sample (Figure 5a). These patterns represent the melt pool, which was also seen along the scanning direction (xy-direction) as in Figure 5b. A cell-like structure with coarse grains was also observed in Figure 5. The microstructure consists of an α -Al matrix (darker in color) surrounded by a fibrous Si eutectic network (lighter in color) (Özer *et al.* 2020).

On the other hand, the hardness of the as-printed sample was about 115.2 ± 7.66 HV, which is higher than that of the as-cast sample (58.6 ± 1.14 HV). This is attributed to its finer microstructure. Smaller grains indicate denser grain boundaries, which block dislocation movement and strengthen the material (Aboulkhair *et al.* 2016).

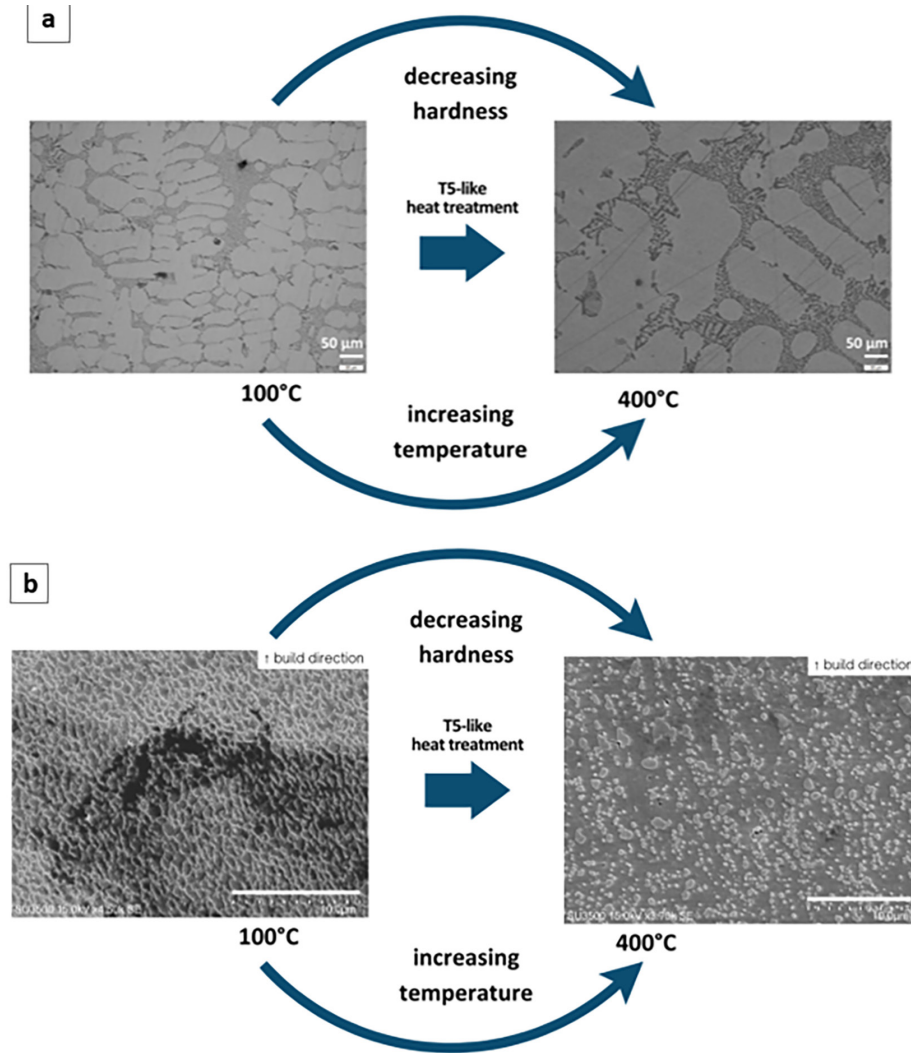


Figure 4. Effect of T5-like heat treatment on the microstructure and hardness of [a] cast A356 samples and [b] 3D-printed AlSi10Mg samples.

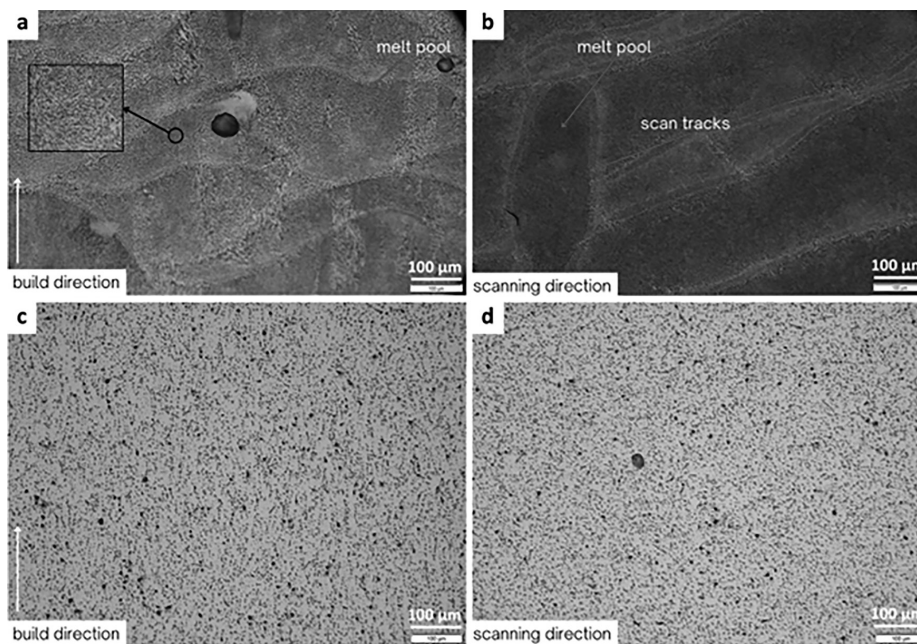


Figure 5. Optical micrographs of the 3D-Printed AlSi10Mg sample [a–b] before and [c–d] after T6-like heat treatment; (left) build direction; (right) scanning direction.

Table 2. Hardness for 3D-printed AlSi10Mg alloy before and after T6-like and T5-like heat treatment.

Sample	Treatment conditions	Hardness at each indentation point					Average hardness (HV 200gf)	
		1	2	3	4	5		
3D-printed Al-Si10Mg Alloy	As-printed (untreated)	z ¹	108	120	106	119	123	115.2 ± 7.66
		xy ²	108	111	104	109	111	108.6 ± 2.88
	After T6-like (ASTM)	z ¹	96	94	102	96	94	96.4 ± 3.29
		xy ²	96	95	98	97	96	96.4 ± 1.14
	After T6-like (EOS)	z ¹	115	110	111	107	106	109.8 ± 3.56
		xy ²	111	108	113	108	109	109.8 ± 2.17
	After T5-like at 100 °C	z ¹	103	111	108	116	110	109.6 ± 4.72
		xy ²	111	113	114	115	120	114.6 ± 3.36
	After T5-like at 200 °C	z ¹	115	117	117	115	116	116 ± 1.00
		xy ²	119	115	122	123	119	119.6 ± 3.13
	After T5-like at 300 °C	z ¹	79	76	76	81	82	78.8 ± 2.77
		xy ²	85	85	82	86	83	84.2 ± 1.64
	After T5-like at 400 °C	z ¹	54	56	56	56	56	55.6 ± 0.89
		xy ²	60	61	61	60	60	60.4 ± 0.55

After T6-like heat treatment (ASTM International 2012), the wave-like patterns in the build direction and the elongated shapes in the scanning direction disappeared. Only quasi-spherical particles uniformly distributed in the microstructure were observed (Figures 5c–d). In addition, after statistical analysis through a t-test for the hardness values in Table 2, a significant decrease from 115.2 ± 7.66 to 96.4 ± 3.29 HV in the build direction and from 108.6 ± 2.88 to 96.4 ± 1.14 HV in the scanning direction was determined. A t-test was conducted with an alpha value (significance level) of $\alpha = 0.05$. This analysis compared paired samples before and after the T6-like heat treatment. Several factors possibly contributed to the decreased hardness after T6-like treatment. First, the solutionizing step possibly degraded the fibrous Si eutectic network, which strengthens the material (Girelli *et al.* 2019; Aboulkhair *et al.* 2016). Second, the internal stresses in the as-built structure were also released after the heat treatment (Girelli *et al.* 2019; Aboulkhair *et al.* 2016). Consequently, the hardness was reduced.

Figure 4b illustrates the effect of T5-like heat treatment on the microstructure and hardness of the 3D-printed AlSi10Mg alloy. At 100 °C, the SEM micrograph of the 3D-printed AlSi10Mg alloy shows an interconnected eutectic Si network consisting of supersaturated Al with Si-rich regions along its boundaries (Figures 6a and 7a). A slight decrease in hardness was also observed. At 200 °C (Figures 6b and 7b), there was no remarkable change in the microstructure, but the hardness slightly increased. Rosenthal and Stern (2016) observed that T5-like heat treatment of AlSi10Mg alloy at 100–170 °C led

to particle coarsening, slightly decreasing the hardness. However, when the temperature was raised to 200–220 °C, precipitates started to form. As a result, a mild increase in the hardness was observed. This phenomenon was also evident in this work.

On the other hand, at 300 °C (Figures 6c and 7c), the interconnected eutectic network starts to break apart, leading to a significant decrease in hardness (from 115.2 ± 7.66 to 78.8 ± 2.77 HV). Fiocchi *et al.* (2020) observed that exposure to temperatures ranging from 240–290 °C leads to the coarsening and spheroidizing of precipitates. Though no spherical particles were evident in the microstructure in this work, the breakup of the eutectic network at 300 °C contributed to the considerable reduction in the hardness. This variation can be attributed to differences in processing parameters that can affect the thermal history of the sample (Žaba *et al.* 2022; Fiocchi *et al.* 2020). Lastly, at 400 °C, the eutectic network completely disappeared (Figures 6d and 7d). Coarse spherical precipitates were finally observed, leading to the lowest hardness value. Further, the microstructure at z- and xy-directions have similar hardness values at 400 °C.

SUMMARY AND CONCLUSION

This study investigated the effects of the T6-like and T5-like heat treatment on the microstructure of Al-Si-Mg alloy systems. Cast A356 alloy was fabricated through traditional casting, and 3D-printed AlSi10Mg alloy was produced through DMLS. The microstructural

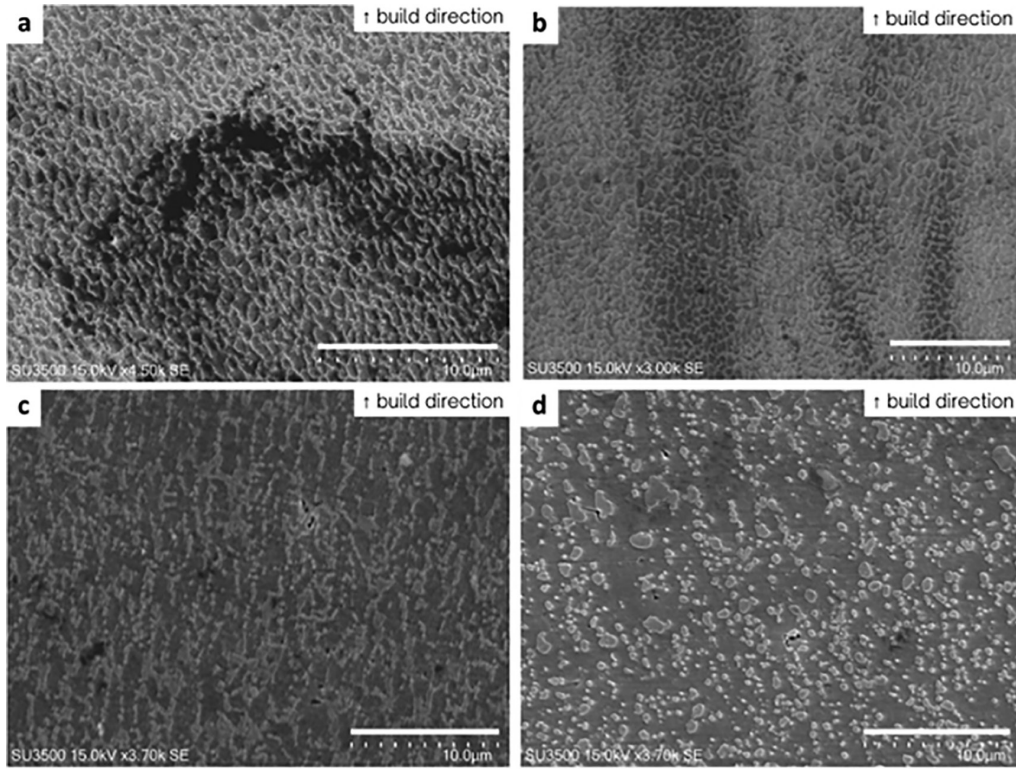


Figure 6. SEM micrographs of 3D-Printed AlSi10Mg sample after T5-like heat treatment at [a] 100, [b] 200, [c] 300, and [d] 400 °C in the build direction (z-direction).

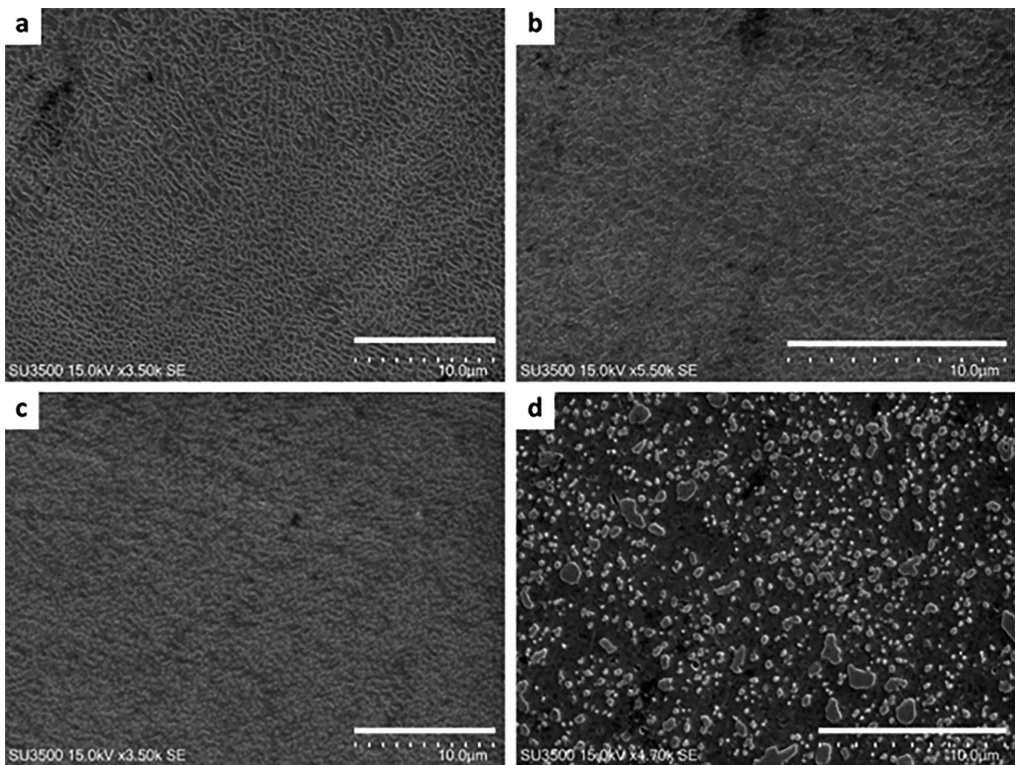


Figure 7. SEM micrographs of 3D-Printed AlSi10Mg sample after T5-like heat treatment at [a] 100, [b] 200, [c] 300, and [d] 400 °C in the scanning direction (xy-direction).

investigation was done through optical microscopy and SEM. Vickers hardness test was conducted to obtain the hardness. Statistical analysis through a t-test was performed to determine the significance of the difference in the hardness values. A number of conclusions were drawn as follows.

[1] The microstructure of the as-cast A356 alloy exhibits an α -Al with an interdendritic Al-Si eutectic. Upon T6-like heat treatment, it retained its dendritic morphology, but the hardness increased from 58.6 ± 1.14 to 85.6 ± 13.63 HV. This is attributed to the formation and growth of precipitates due to solutionizing near the eutectic temperature, quenching, and artificial aging. Upon T5-like heat treatment, the hardness continuously decreased upon direct exposure to elevated temperatures. The microstructure, however, did not exhibit significant visible changes.

[2] The microstructure of the as-printed AlSi10Mg alloy showed wave-like patterns in the build direction (z-direction) corresponding to the melt pools formed during the DMLS process. In the scanning direction (xy-direction), scan tracks that correspond to the melt pool boundaries were observed. It also exhibited a fibrous Si eutectic network around the α -Al. Upon T6-like heat treatment, the coarsening of precipitates was observed, and the melt pools and scan tracks nearly disappeared in the microstructure. This affects the hardness of the alloy, which decreased from 115.2 ± 7.66 to 96.4 ± 3.29 HV in the z-direction. Upon T5-like heat treatment at lower temperatures (100 and 200 °C) the eutectic network remained intact, but eventually disappeared at higher temperatures (300 and 400 °C). The hardness also significantly decreased to 55.6 ± 0.89 HV at 400 °C.

[3] The effects of T6-like heat treatment on the cast and 3D-printed Al-Si-Mg alloys were evidently different: hardness values for the cast sample significantly increased, whereas that of the 3D-printed sample decreased. This difference in response is mainly attributed to the inherently fine microstructure of the 3D-printed sample as a result of the DMLS process. This also accounts for the higher hardness value of the 3D-printed sample in its untreated state (115.2 ± 7.66 HV) as compared to the hardness of the cast sample with its improved hardness (85.6 ± 13.63 HV) after T6-like heat treatment.

[4] The effect of T5-like heat treatment on the cast and 3D-printed Al-Si-Mg alloys was similar. For the 3D-printed samples, statistical analysis through a t-test revealed no significant difference in the hardness after T5-like heat treatment at the lower temperatures (100 and 200 °C). However, the hardness significantly decreased at higher temperatures (300 and 400 °C).

ACKNOWLEDGMENTS

The authors gratefully acknowledge the Department of Science and Technology's Advanced Manufacturing Center or DOST-AMCen under the Metals Industry Research and Development Center or DOST-MIRDC for providing the 3D-printed and cast samples, respectively, as well as the undergraduate thesis grant provided by the University of the Philippines Engineering Research and Development Foundation, Inc. or UPERDFI through the College of Engineering of the University of the Philippines Diliman.

STATEMENT ON CONFLICT OF INTEREST

There are no conflicts to declare.

REFERENCES

- ABOULKHAIRNT, MASKERYI, TUCK C, ASHCROFT I, EVERITT NM. 2016. The microstructure and mechanical properties of selectively laser melted AlSi10Mg: the effect of a conventional T6-like heat treatment. *Mater Sci Eng A* 667: 139–146.
- ABOULKHAIRNT, TUCK C, ASHCROFT I, MASKERY I, EVERITT NM. 2015. On the precipitation hardening of selective laser melted AlSi10Mg. *Metall Mater Trans A* 46: 3337–3341.
- ALKATHAFI MH, KHALIL AA, ABDALLA AO. 2020. The effect of cooling rate on the microstructure of A356 aluminium alloy. *SVOA Materials Science & Technology* 2(04): 91–99.
- ASTM INTERNATIONAL. 2012. ASTM F2792-12a: standard terminology for additive manufacturing technologies. West Conshohocken, PA.
- BIROL Y. 2009. Response to artificial ageing of dendritic and globular Al-7Si-Mg alloys. *Journal of Alloys and Compounds* 484(1–2): 164–167. <https://doi.org/10.1016/j.jallcom.2009.05.043>
- CHERDO L. 2019. The best metal 3D printers in 2019. Accessed on 23 Aug 2019 at <https://www.aniwaa.com/best-of/3d-printers/best-metal-3d-printer/>
- CHAUDHURY SK, WARKE V, SHANKAR S, APELIAN D. 2011. Localized recrystallization in cast Al-Si-Mg alloy during solution heat treatment: dilatometric and calorimetric studies. *Metall Mater Trans A* 42: 3160–3169.

- CHAUHAN K. 2017. Influence of heat treatment on the mechanical properties of aluminium alloys (6xxx Series): a literature review. *Inter J Eng Res* 6: 386–389.
- DEV SINGH D, MAHENDER T, RAJI REDDY A. 2021. Powder bed fusion process: a brief review. *Mater Today Proceed* 46: 350–355.
- EOS. 2021. EOS M 290 simply production of metal parts.
- FIOCCHI J, BIFFI CA, COLOMBO C, VERGANI LM, TUISSI A. 2020. *Ad hoc* heat treatments for selective laser melted AlSi10Mg alloy aimed at stress-relieving and enhancing mechanical performances. *JOM* 72: 1118–1127.
- FIOCCHI J, TUISSI A, BIFFI CA. 2021. Heat treatment of aluminium alloys produced by laser powder bed fusion: a review. *Mater Des* 204: 109651.
- GIRELLI L, TOCCIM, GELFIM, POLAA. 2019. Study of heat treatment parameters for additively manufactured AlSi10Mg in comparison with corresponding cast alloy. *Mater Sci Eng A* 739: 317–328.
- KIM W, JANG K, JI C, LEE E. 2021. Effects of heat treatment on the microstructure and hardness of A356 (AlSi7Mg0.3) manufactured by vertical centrifugal casting. *App Sci* 11: 11572.
- LEE CD. 2013. Effect of T6 heat treatment on the defect susceptibility of fatigue properties to microporosity variations in a low-pressure die-cast A356 alloy. *Mater Sci Eng A* 559: 496–505.
- LIU G, WANG Q, LIU T, YE B, JIANG H, DING W. 2017. Effect of T6 heat treatment on microstructure and mechanical property of 6101/A356 bimetal fabricated by squeeze casting. *Mater Sci Eng A* 696: 208–215.
- ÖZER G, TARAKÇI G, YILMAZ MS, ÖTER Z, SÜRMEŒ Ö, AKÇAY, COŞKUN M, KOÇ E. 2020. Investigation of the effects of different heat treatment parameters on the corrosion and mechanical properties of the AlSi10Mg alloy produced with direct metal laser sintering. *Mater Corr* 71: 365–373.
- PILLER FT, POPRAWA R, SCHLEIFENBAUM HJ, SCHUH G, BARG S, DOLLE C, HINKE C, JANK MH, JIANG R, MEINERS W, RIESENER M, SCHRAGE J, ZIEGLER S. 2018. Introducing a holistic profitability model for additive manufacturing: an analysis of laser-powder bed fusion. *Proceeding of the IEEE International Conference on Industrial Engineering and Engineering Management*; 16–19 Dec 2018; Bangkok, Thailand. p. 1730–1735.
- ROSENTHAL I, STERN A. 2016. Heat treatment investigation of the AlSi10Mg alloy produced by selective laser melting (SLM): microstructure and hardness. *Annals “Dunarea de Jos” Univ Galati Fascicle XII: Welding Equipment and Technology* 27: 7–11.
- TAMEZ MAB, TAHA I. 2021. A review of additive manufacturing technologies and markets for thermosetting resins and their potential for carbon fiber integration. *Add Manufac* 37: 101748.
- YU X, WANG L. 2018. T6 heat-treated AlSi10Mg alloys additive-manufactured by selective laser melting. *Proc Manufac* 15: 1701–1707.
- ŹABA K, TUZ L, NOGA P, RUSZ S, ZABYSTRZAN R. 2022. Effect of multi-variant thermal treatment on microstructure evolution and mechanical properties of AlSi10Mg processed by direct metal laser sintering and casting. *Mater* 15: 974.
- ZHU M, JIAN Z, YANG G, ZHOU Y. 2012. Effects of T6 heat treatment on the microstructure, tensile properties, and fracture behavior of the modified A356 alloys. *Mater Des* 36: 243–249.